CHEMICAL ENGINEERING TRANSACTIONS
VOL. 42, 2014
A publication of AIDIC
The Italian Association of Chemical Engineering
www.aidic.it/cet
Guest Editors: Petar Sabev Varbanov, Neven Duić

ISBN 978-88-95608-33-4; **ISSN** 2283-9216
DOI:10.3303/CET1442016

Technical Damage in Wind Rotor Blade under Static Load at Environment Conditions

Wilfried Becker[a], Varbinka Valeva[b], Tatyana Petrova[c], Jordanka Ivanova*[b]

[a]Technical University of Darmstadt, Darmstadt, Germany
[b]Institute of Mechanics, Bulgarian Academy of Sciences, Acad. G. Bontchev str., bl. 4, Sofia, Bulgaria
[c]Institute of Chemical Engineering, Bulgarian Academy of Sciences, Acad. G. Bontchev str., bl.103, Sofia, Bulgaria
ivanova@imbm.bas.bg

Accidents with a wind rotor blade are frequently observed in the wind farms and the simulation study of its undesired damage and its full degradation has to be done. As usual the full degradation of the wind rotor blade happens in a sequence of appearing first transitive (I mode crack) and then interface delamination (II mode crack) between the involved layers of a rotor blade laminate. The question of the risk value of the interface delamination is important for further reliability of wind blade to work safety.
In the present approach the unacceptable interface delamination in a pre-cracked (1st mode) bi-material structure as a part of the straight line of wind rotor blade under static mechanical, temperature, and electric loading and moisture will be considered. With this first step, the influence of environment conditions such as moisture and temperature as well as the properties of the bi-material plate will be assumed to be linear.
The investigation will be performed by using a simple 1D shear lag model of the unit cell of wind rotor blade. The electric voltage acting on the first piezoelectric plate of bi-material structure will be used as a sensor identifying the possible delamination between the layers. The material and physical properties of the structure are taken from literature. The obtained results are illustrated by figures and discussed. Some recommendations for safety work of the wind rotor blade as well as a criterion for identifying the interface delamination through the electric gradient will be proposed.

1. Introduction

A composite material under coupled or uncoupled effects of four fields - mechanical, electrical, thermal, and moisture is considered as a hygrothermopiezoelectric medium. In fact, piezoelectricity takes into account the interaction between elastic and electric fields. Beyond that the hygrothermoelasticity theory describes the behaviour of piezoelectric solids under the influences of temperature field and absorption of moisture. Adaptive piezoelectric composite structures, subjected to environmental effects are examples of such a medium.
The theory of thermopiezoelectricity (Mindlin, 1974) describes the behaviour of a solid under the coupled effects of elastic, electric, and temperature fields. The effects of the four fields (elastic, electric, temperature and moisture) on laminated composites have been studied separately but there are not enough examples where these effects are studied simultaneously. An exact solution in three dimensions for a simply supported rectangular laminated elastic plate was derived by Pagano (1970). Piezoelectric and thermopiezoelectric effects were incorporated to yield exact solutions for static analysis of laminated composites (Ray et al., 1993), as well as for laminated beams (Heyliger, 1997). The discrete-layer models, using the layer wise theories, were developed for analysing laminated piezoelectric plates (Heyliger et al., 1994) and further to carry out their dynamic analysis (Saravanos et al., 1997). However, none of these studies has considered the four fields combined. A very complete mathematical theory of hygrothermoelasticity has been presented in the work by Sih et al. (1986) as well as by Suhir (1989).
In the paper of Johansson (2013) the author wrote, “Renewable energy (RE) sources are closely related to climate conditions. Examples of factors that will impact RE are changes in temperature, wind patterns, cloudiness and the hydrological cycle.” On the other hand the accidents with wind rotor blades (Caithness Wind farm Information Forum, 2013) show that the problem with safety work of wind rotor blades becomes very important (Figure 1). So, the motivation of the present paper is the investigation of important environmental conditions on the work of the

Please cite this article as: Becker W., Valeva V., Petrova T., Ivanova J., 2014, Technical damage in wind rotor blade under static load at environment conditions, Chemical Engineering Transactions, 42, 91-96 DOI:10.3303/CET1442016

wind turbine blade. Encouraged by the excellent performance of the shear lag method in the case of static and dynamic loading of preliminary damaged bi-material structures (Gambin et al., 2011), the authors of the present paper applied this method to investigate the piezoelastic response with the influence of moisture and a temperature field of a bi-material structure with possible delamination along the interface. The validation of the shear lag method was confirmed with some experimental data in the paper (Nikolova et al., 2009). The comparisons show very good agreement up to 7 %.

In the present paper the authors will model the idealized straight line part of a wind rotor blade by an analytical and simple 1D shear lag model and will analyse and detect the possible interface delamination through the change of the voltage, temperature and moisture for the hygrothermopiezoelectric bi-material structure at steady state behaviour. Additionally, some recommendation for an optimal choice of material, geometrical, physical and loading characteristics is proposed on the base of satisfying certain conditions. This study could help to observe and prevent technical damage of wind rotor blade.

2. Statement of the problem

The shear lag method has been known from the assumptions proposed by Cox, (1952). Among the engineering society, this method became a common computational tool for analytical stress analysis in composite materials, especially for new wind blade materials containing the carbon fibres (Saelhof A-K et al., 2013). The main idea of the shear-lag analysis is the assumption which involves a simplification of in-plane shear stress and decouples the 2D problem into two 1D ones. In the shear lag model the hypothesis that the load is transferred from broken fibres to adjacent ones by the matrix shear force is stated. Hence, the matrix shear force is independent of the transverse displacements.

It is assumed that the wind rotor blade consists in a regular repetition along the longitudinal direction of a bi-material plate configuration with different material properties, so the structure can be considered as a composite represented by a unit cell. The shear lag analysis will be applied to the model of the unit 2D bi-material cell according to Figure 2, where by $2h_\alpha$ $(\alpha=A, B)$, $2l$, $2l_e$, T, H the thicknesses of the plates A and B, the length of the unit cell, the debonding length, and the temperature and moisture concentration change are indicated, respectively. The external mechanical load is applied as ε_0, while the electric field is given by the electric displacement D_0. The static statement is a first step in our investigation. The importance of such an approach is connected with the large tensile stresses, arising in the working blade.

According to materials used in a wind rotor blade, it is assumed that the first plate A is transversal isotropic elastic with piezoelectric properties and sensitive to thermal effects. The second plate B is in general transversal isotropic, sensitive to thermal and moisture effects. Both plates are connected with a zero thickness isotropic elastic material line with a shear modulus G_I, (interface I) working only on shear, while both plates work on extension. Any bending is neglected.

To obtain the 1D system differential equations at assumption of shear lag hypothesis we start from 3D case according to Eq(1). Hygrothermopiezoelectric steady state interface behaviour of a solid structure (uncoupled 3D problem) is posed using the following system of differential equations:

$$\sigma_{ij,j}=0 \qquad D_{i,i}=0 \qquad T_{,ii}=0 \qquad H_{,ii}=0 \qquad (i,j=1,2,3) \tag{1}$$

where by Eq(1/3) (the “Eq(1/3)” denotes the third equation from Eq(1)) and Eq(1/4) the heat and moisture flux equations with absence of sources are indicated. Bellow in the text the numbering of equations follows the same meaning. The subscript “ii” denotes the double differentiation by coordinates of respective electric, temperature and moisture functions; by σ_{ij}, D_i the tensor of stresses and electric displacement vector are denoted. The following reduced constitutive equations are obtained for the model, given by Figure 2:

$$\sigma_x^A=c_{11}^{*A}\varepsilon_x^A-e_{31}^{*A}E_z^A-\alpha_{11}^{*A}T-\beta_{11}^{*A}H \tag{2}$$

$$\sigma_x^B=c_{11}^{*B}\varepsilon_x^B-\alpha_{11}^{*B}T-\beta_{11}^{*B}H \tag{3}$$

$$D_z^A=e_{31}^{*A}\varepsilon_x^A+\varepsilon_{33}^{*A}E_z^A+p_3^{*A}T+q_3^{*A}H \tag{4}$$

$$c_{11}^{*\alpha}=c_{11}^{\alpha}-\left[(c_{11}^{\alpha})^2c_{33}^{\alpha}-2c_{12}^{\alpha}c_{13}^{\alpha}c_{23}^{\alpha}+(c_{13}^{\alpha})^2c_{22}^{\alpha}\right]/\left[c_{22}^{\alpha}c_{33}^{\alpha}-(c_{23}^{\alpha})^2\right] \tag{5}$$

$$e_{31}^{*A}=e_{31}^{A}-\left[e_{32}^{A}(c_{12}^{A}c_{33}^{A}-c_{13}^{A}c_{23}^{A})+e_{33}^{A}(c_{13}^{A}c_{22}^{A}-c_{12}^{A}c_{23}^{A})\right]/\left[c_{22}^{\alpha}c_{33}^{\alpha}-(c_{23}^{\alpha})^2\right] \tag{6}$$

$$\varepsilon_{33}^{*A}=\varepsilon_{33}^{A}+\left[e_{32}^{A}(c_{33}^{A}e_{32}^{a}-c_{23}^{A}e_{33}^{a})+e_{33}^{A}(c_{22}^{A}e_{33}^{a}-c_{23}^{A}e_{32}^{a})\right]/\left[c_{22}^{a}c_{33}^{a}-(c_{23}^{a})^{2}\right] \quad (7)$$

$$\alpha_{11}^{*a}=\alpha_{11}^{a}-\left[\alpha_{22}^{a}(c_{12}^{a}c_{33}^{a}-c_{13}^{a}c_{23}^{a})+\alpha_{33}^{a}(c_{13}^{a}c_{22}^{a}-c_{12}^{a}c_{23}^{a})\right]/\left[c_{22}^{a}c_{33}^{a}-(c_{23}^{a})^{2}\right] \quad (8)$$

$$\beta_{11}^{*a}=\beta_{11}^{a}-\left[\beta_{22}^{a}(c_{12}^{a}c_{33}^{a}-c_{13}^{a}c_{23}^{a})+\beta_{33}^{a}(c_{13}^{a}c_{22}^{a}-c_{12}^{a}c_{23}^{a})\right]/\left[c_{22}^{a}c_{33}^{a}-(c_{23}^{a})^{2}\right] \quad (9)$$

$$p_{3}^{*A}=p_{3}^{A}+\left[\alpha_{22}^{A}(c_{33}^{A}e_{32}^{a}-c_{23}^{A}e_{33}^{a})+\alpha_{33}^{A}(c_{22}^{A}e_{33}^{a}-c_{23}^{A}e_{32}^{a})\right]/\left[c_{22}^{a}c_{33}^{a}-(c_{23}^{a})^{2}\right] \quad (10)$$

$$q_{3}^{*A}=q_{3}^{A}+\left[\beta_{22}^{A}(c_{33}^{A}e_{32}^{a}-c_{23}^{A}e_{33}^{a})+\beta_{33}^{A}(c_{22}^{A}e_{33}^{a}-c_{23}^{A}e_{32}^{a})\right]/\left[c_{22}^{a}c_{33}^{a}-(c_{23}^{a})^{2}\right] \quad (11)$$

where σ_x^a and ε_x^a are stresses and strains for the respective layers; c_{ij}^a, e_{ij}^A, ε_{ij}^A, α_{ij}^A, β_{ij}^A, p_3^A, q_3^A $(a=A, B)$ $(i, j=1, 2, 3)$ are independent elastic constants (measured at constant electric field), piezoelectric and dielectric constants (measured at constant strain), thermal and moisture stress coefficients, pyroelectric and hygroelectric coefficients, respectively. Again, note that the electric field acts along the axis Oz, while the mechanical load acts along the axis Ox (Figure 2).

Figure 1: Blade delamination

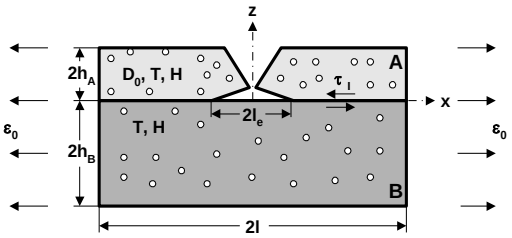

Figure 2: Model of the unit cell of bi-material in wind blade structure

The following constitutive equations hold for the electric gradient Eq(12/4) and the stresses within the plates A and B Eq(12/1) and Eq(12/2) as well as Eq(12/3) for the interface:

$$\sigma_x^A=\sigma_A=\left(c_{11}^{*A}-\frac{(e_{31}^{*A})^2}{\varepsilon_{33}^{*A}}\right)\frac{du_A}{dx}-\frac{e_{31}^{*A}}{\varepsilon_{33}^{*A}}D_z^A-\left(\alpha_{11}^{*A}-\frac{e_{31}^{*A}}{\varepsilon_{33}^{*A}}p_3^{*A}\right)T-\left(\beta_{11}^{*A}-\frac{e_{31}^{*A}}{\varepsilon_{33}^{*A}}q_3^{*A}\right)H \quad (12)$$

$$\sigma_x^B=\sigma_B=c_{11}^{*B}\frac{du_B}{dx}-\alpha_{11}^{*B}T-\beta_{11}^{*B}H \qquad \tau_I=G_I\frac{u_A-u_B}{h_A+h_B} \qquad E_z^A=\frac{D_z^A}{\varepsilon_{33}^{*A}}-\frac{e_{31}^{*A}}{\varepsilon_{33}^{*A}}\frac{du_A}{dx}-\frac{p_3^{*A}}{\varepsilon_{33}^{*A}}T-\frac{q_3^{*A}}{\varepsilon_{33}^{*A}}H$$

The kinematic behaviour within the plates is given by $\varepsilon^{tot}=du/dx$ and $\varepsilon^{mech}=\varepsilon^{tot}-\varepsilon^{pzel}-\varepsilon^{T}-\varepsilon^{H}$. According to the shear lag hypothesis (Ivanova et al., 2010), the system of differential equations for the equilibrium of the unit cell (Figure 2) is given as follows:

$$\frac{d\sigma_A}{dx}-\frac{\tau_I}{2h_A}=0 \qquad \frac{d\sigma_B}{dx}+\frac{\tau_I}{2h_B}=0 \qquad \frac{dD_z^A}{dz}=0 \qquad \frac{d^2T}{dx^2}=0 \qquad \frac{d^2H}{dx^2}=0 \quad (13)$$

where the solution $D_z^A=D_0$ $(0\le x\le l)$ of the third equation from Eq(4) can be easily obtained. The integration of the last two equations of Eq(4) gives $T=T_1-(T_1-T_0)(1-x/l)$ and $H=H_1-(H_1-H_0)(1-x/l)$. Boundary and contact conditions are given as follows:

$$\varepsilon^{A,B}(l)=\varepsilon_0 \qquad u_B(0)=0 \qquad \sigma(0)=0 \qquad T(0)=T_0 \qquad T(l)=T_1 \qquad H(0)=H_0 \qquad H(l)=H_1 \quad (14)$$

The general solution of Eq(13) together with Eq(14) for the hygrothermopiezoelastic stresses and displacements is obtained and is given by following expressions:

$$u_A=\frac{1}{\lambda}\left(\varepsilon_0-\frac{R}{\lambda^2}l\right)\left\{\frac{ch[\lambda(l-x)]}{sh(\lambda l)}+\left(\frac{\lambda^2}{\xi}-1\right)\frac{ch(\lambda l)}{sh(\lambda l)}+(\lambda x)\right\}-\frac{1}{\xi}\left(P-\frac{R}{\lambda^2}\right)+\frac{R}{\lambda^2}\frac{x^2}{2} \quad (15)$$

$$u_B=\frac{1}{\lambda}\left(\varepsilon_0-\frac{R}{\lambda^2}I\right)\left\{\left(1-\frac{\lambda^2}{\xi}\right)\frac{ch[\lambda(l-x)]-ch(\lambda l)}{sh(\lambda l)}+(\lambda x)\right\}+\frac{R}{\lambda^2}\frac{x^2}{2} \tag{16}$$

$$\sigma_A=\left(c_{11}^{*A}+\frac{(e_{31}^{*A})^2}{\varepsilon_{33}^{*A}}\right)\left\{\left(\varepsilon_0-\frac{R}{\lambda^2}I\right)\left[1-\frac{sh[\lambda(l-x)]}{sh(\lambda l)}\right]+\frac{R}{\lambda^2}x\right\}-\frac{e_{31}^{*A}}{\varepsilon_{33}^{*A}}D_0 \tag{17}$$

$$-\left(\alpha_{11}^{*A}-\frac{e_{31}^{*A}}{\varepsilon_{33}^{*A}}p_3^{*A}\right)\left[T_1-(T_1-T_0)\left(1-\frac{x}{l}\right)\right]-\left(\beta_{11}^{*A}-\frac{e_{31}^{*A}}{\varepsilon_{33}^{*A}}q_3^{*A}\right)\left[H_1-(H_1-H_0)\left(1-\frac{x}{l}\right)\right]$$

$$\sigma_B=c_{11}^{*B}\left\{\left(\varepsilon_0-\frac{R}{\lambda^2}I\right)\left[1-\frac{sh[\lambda(l-x)]}{sh(\lambda l)}\left(1-\frac{\lambda^2}{\xi}\right)\right]+\frac{R}{\lambda^2}x\right\}-\alpha_{11}^{*B}\left[T_1-(T_1-T_0)\left(1-\frac{x}{l}\right)\right]-\beta_{11}^{*B}\left[H_1-(H_1-H_0)\left(1-\frac{x}{l}\right)\right] \tag{18}$$

$$\tau_l=\frac{G_l}{(h_A+h_B)}\frac{1}{\xi}\left\{\lambda\left(\varepsilon_0-\frac{R}{\lambda^2}I\right)\frac{ch[\lambda(l-x)]}{sh(\lambda l)}+\frac{R}{\lambda^2}-P\right\} \tag{19}$$

$$E_z^A=\frac{D_0}{\varepsilon_{33}^{*A}}-\frac{e_{31}^{*A}}{\varepsilon_{33}^{*A}}\left\{\left(\varepsilon_0-\frac{R}{\lambda^2}I\right)\left[1-\frac{sh[\lambda(l-x)]}{sh(\lambda l)}\right]+\frac{R}{\lambda^2}x\right\}-\frac{p_3^{*A}}{\varepsilon_{33}^{*A}}\left[T_1-(T_1-T_0)\left(1-\frac{x}{l}\right)\right]-\frac{q_3^{*A}}{\varepsilon_{33}^{*A}}\left[H-(H_1-H_0)\left(1-\frac{x}{l}\right)\right] \tag{20}$$

where $\lambda^2=\xi+\eta>0$ and the coefficients in Eqs(15-20) are:

$$\xi=\frac{1}{2h_A(h_A+h_B)}\left\{G_l\Big/\left(c_{11}^{*A}+\frac{(e_{31}^{*A})^2}{\varepsilon_{33}^{*A}}\right)\right\} \qquad Q=\frac{\alpha_{11}^{*B}}{c_{11}^{*B}}\frac{1}{l}(T_1-T_0)+\frac{\beta_{11}^{*B}}{c_{11}^{*B}}\frac{1}{l}(H_1-H_0)$$

$$\eta=\frac{1}{2h_B(h_A+h_B)}\frac{G_l}{c_{11}^{*B}} \qquad P=\frac{\left(\alpha_{11}^{*A}-\frac{e_{31}^{*A}}{\varepsilon_{33}^{*A}}p_3^{*A}\right)}{\left(c_{11}^{*A}+\frac{(e_{31}^{*A})^2}{\varepsilon_{33}^{*A}}\right)}\frac{1}{l}(T_1-T_0)+\frac{\left(\beta_{11}^{*A}-\frac{e_{31}^{*A}}{\varepsilon_{33}^{*A}}q_3^{*A}\right)}{\left(c_{11}^{*A}+\frac{(e_{31}^{*A})^2}{\varepsilon_{33}^{*A}}\right)}\frac{1}{l}(H_1-H_0) \tag{20}$$

The length of an interfacial debonding is found from the assumption that the interface shear stress reaches its failure limit τ^{cl}, i.e. $\tau_l(l_e)=\tau^{cl}$. According to Eq(19) the following equation is found and is solved with respect to the debond length l_e:

$$ch[\lambda(l-l_e)]=\left\{sh(\lambda l)/\lambda\left(\varepsilon_0-\frac{R}{\lambda^2}I\right)\right\}\left[\frac{(h_A+h_B)\xi}{G_l}\tau^{cr}-\frac{R}{\lambda^2}+P\right] \tag{21}$$

The solution of Eq(21) is given by

$$l_e=l-\frac{1}{\lambda}\ln\left(C\pm\sqrt{C^2-1}\right) \qquad C=\left\{sh(\lambda l)/\lambda\left(\varepsilon_0-\frac{R}{\lambda^2}I\right)\right\}\left[\frac{(h_A+h_B)\xi}{G_l}\tau^{cr}-\frac{R}{\lambda^2}+P\right] \tag{22}$$

Let us consider the region of definition of the obtained solution Eq(22) for the debond length and the coefficient C. Important is to note, that since C is a function of geometry, mechanical and physical characteristics of the bi-material structure, as well as of the mechanical load, the value of C has to be calculated before starting numerical calculations. Calculating the coefficient C at constant geometry and mechanical and electric loading one can vary and choose mechanical and physical properties of the bi-material structure in order to find a more reliable structure with respect to the interface delamination. To have the real solution for the debond length, the following conditions have to be satisfied: $C\geq 1$ and $C\leq[\exp(2\lambda l)+1]/2\exp(\lambda l)$. On the other side when $C=1$, the full unacceptable degradation of the interface appears, i.e. $l_e=l$, while if $C=[\exp(2\lambda l)+1]/2\exp(\lambda l)$ there is not any delamination along the interface, i.e. $l_e=0$. So, the possible recommendations for safety work of the wind rotor blade without appearance of any interface delamination between layers is the right combination of geometry, material and loading by satisfying the condition $C=[\exp(2\lambda l)+1]/2\exp(\lambda l)=1$.

3. Numerical example

The geometry, the mechanical and electric loads, the interface material properties as well as the temperatures and moisture concentrations are assumed to be given as follows:

l=140 mm, h_A=2 mm, h_B=5 mm, ε_0=0.1%÷2%, G_l=800 MPa, τ^{cr}=18 MPa,
D_0=0.5 C/m^2, T_0=200 K, T_1=330 K, H_0=0.5 wt.%, H_1=5.0 wt.%

The material, piezoelectric, thermal and moisture characteristics for the plate materials are given in Table 1. PZT-4 and Wood are taken from (Smittakorn, 2001) and respectively for IM7/8552 from (Liljedahl et al., 2007). The following cases of material and physical characteristics of the plates A and B are considered:

Case 1: plate A – piezo-elastic, plate B – elastic,
Case 2: plate A – piezo-thermo-elastic, plate B – hygro-thermo-elastic.

Table 1: Properties of the materials

Characteristics and Units	Symbols used	PZT-4	Wood	IM7/8552
Elastic constants (GPa)	c_{11}	139.0	12.22	172.0
	c_{22}	139.0	0.6699	13.67
	c_{33}	115.0	1.273	13.67
	c_{12}, c_{21}	77.8	0.4682	6.48
	c_{13}, c_{31}	74.3	0.6872	6.48
	c_{23}, c_{32}	74.3	0.0905	7.227
Piezoelectric constants (C/m^2)	e_{13}, e_{31}, e_{23}, e_{32}	-5.20	0	0
	e_{33}	15.08	0	0
Dielectric constants $\times 10^{-10}$ (C/Vm)	ε_{11}, ε_{22}	130.54	0	0
	ε_{33}	115.05	0	0
Pyroelectric coefficients $\times 10^{-6}$ (C/m^2K)	p_1, p_2, p_3	-250.0	0	0
Thermal stress coefficients $\times 10^5$ (N/m^2K)	α_{11}	0.278	0.043	0.103
	α_{22}	0.278	0.027	0.391
	α_{33}	0.230	0.038	0.391
Moisture stress coefficients $\times 10^5 (N/m^2\%)$	β_{11}	0	0	0
	β_{22}	0	0.708	62.88
	β_{33}	0	0.925	62.88

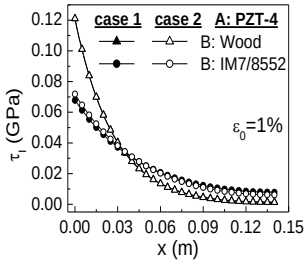

Figure 3: Interface shear stress as a function of x

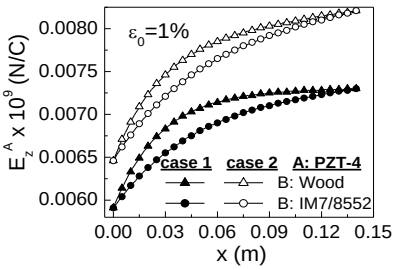

Figure 4: Electric gradient as a function o x *f*

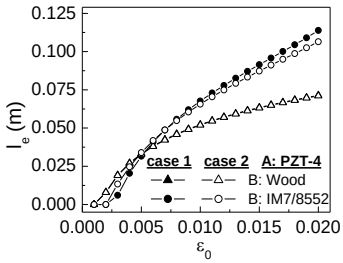

Figure 5: Behavior of the debond length for values of the mechanical load (dimensionless)

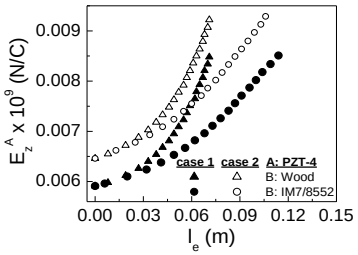

Figure 6: Electric gradient as a function different of the debond length

Figure 3 describes the behaviour of the interface shear stress along the length of the bi-material unit cell at $\varepsilon_0=1\ \%$ for two materials for the plate B: wood and IM7/8552 and for plate A – PZT-4. It can be seen, that the case 1 and case 2 don't differ practically – case 2 covers case 1. Figure 4 shows the behaviour of the electric gradient at the above mentioned conditions. The case 2 differs significantly from the case 1. The presence of moisture and temperature increases the values of the electric gradient. The debond length as shown in Figure 5 grows up with increasing the mechanical load $\varepsilon_0=0.1\ \%\div 2\ \%$.

The indirect dependence of the electric gradient from debond length is shown in Figure 6. A significant influence of the temperature and moisture is observed which is confirmed by (Smittakorn, 2001). Figure 6 presents a possible criterion for identifying the debond length, which states that for every value of the electric gradient the respective debond length corresponds. If the electric gradient can be measured, then the question what is the value of the interface delamination (debond length) is answered. In a real application the first plate plays the role of the sensor and can give the information about interface debond length.

4. Conclusion

The modelling of the idealized straight line part of a wind rotor blade by an analytical and simple 1D shear lag model used to analyse and detect the possible interface delamination through the change of the voltage, temperature and moisture has been presented. The numerical examples show the strong influence of the presence of moisture, which is very important for the possible full degradation of the interface of the bi-material structure, as well as the strong influence from the mechanical properties of the materials of the plate B. The method and modelling allow taking different combinations of the geometry, material, physical parameters (temperature, moisture) and mechanical and electric loadings in order to predict the optimal choice of them for safety work of wind rotor blade without presence of any interface delamination. The results obtained need experimental verification and the authors are going to try to validate the recommendations made in the paper.

Acknowledgements

The authors greatly appreciate the financial support from the contract BE 1090/36-1 “Hygrothermopiezoelectric 1D model for health monitoring of a bi-material structure” with DFG, Germany.

References

Caithness Wind farm Information Forum, 2013, Summary of Wind Turbine Accident data to 31 December 2013, <www.caithnesswindfarms.co.uk/accidents.pdf>, accessed 17/09/2014.

Cox L. H., 1952, The Elasticity and Strength of Paper and Other Fibrous Materials, Brit.J. Appl. Phys., 3, 72.

Gambin B., Ivanova J., Valeva V., Nikolova G., 2011, Precracking and interfacial debonding in a bi-material structure: Static and dynamic loading, Acta Mech. Sin., 27, 80-89.

Heyliger P.R., 1997, Exact Solutions for Simply Supported Laminated Piezoelectric Plates, J. Appl.Mech., 64, 299-306.

Heyliger P.R., Ramirez G., Saravanos D.A., 1994, Coupled Discrete-Layer Finite Element Models for Laminated Piezoelectric Plates, Commun. Numer. Meth. Eng., 10, 971-981.

Ivanova J., Nikolova G., Dineva P., Becker W., 2010, Interface behavior of a bi-material plate under dynamic loading, J. of Engineering Mechanics ASCE, 136,1194-1201.

Johansson B., 2013, Security aspects of future renewable energy system, A short overview, Energy, 61, 598-605.

Liljedahl C.D.M., Crocombe A.D., Wahab M.A., Ashcroft I.A., 2007, Modelling the environmental degradation of adhesively bonded aluminium and composite joints using a CZM approach, The International Journal of Adhesion and Adhesives, 27, 505-518.

Mindlin R.D., 1974, Equations of High Frequency Vibrations of Thermopiezoelectric Crystal Plates, Int. J. Solids Struct., 10, 625-637.

Nikolova G., Ivanova J., 2009, Cracked bi-material plates under thermomechanical loading, Key Eng. Mat., 409, 406-413.

Pagano N.J., 1970, Exact Solutions for Rectangular Bidirectional Composites and Sandwich Plates, J. Composite Mater., 4, 20-34.

Ray M.C., Bhattacharya R., Samata B., 1993, Exact Solutions for Static Analysis of Intelligent Structures, American Institute of Aeronautics and Astronautics Journal, 31, 1684-1691.

Saelhoff A-K, Wilms Ch., Warnecke M., Pico D., Sernecki M., Seide G., Gries Th., 2013, Matrix/fibre reinforced plastics:characterization of the adhesion, Chemical Engineering Transactions, 32, 1633-1638.

Saravanos D.A., Heyliger P.R., Hopkins D.A., 1997, Layerwise Mechanics and Finite Element for the Dynamic Analysis of Piezoelectric Composite Plates, Int. J. Solids Struct., 34, 359-378.

Sih G. C., Michopoulos J.G., Chou S.C., 1986. Hygrothermoelasticity, Martinus Nijhoff Publisher, Dordrecht, The Netherlands.

Smittakorn W., 2001, A theoretical and experimental study of adaptive wood composites, PhD Thesis, Department of Civil Engineering, Colorado State University, Fort Collins, Colorado, USA.

Suhir E., 1989, Interfacial stresses in bi-metal thermostats, J. Appl. Mech. ASME, 56, 595-600.